

AperTO - Archivio Istituzionale Open Access dell'Università di Torino

Non-neurogenic SVZ-like niche in dolphins, mammals devoid of olfaction

This is the author's manuscript

Original Citation:

Availability:

This version is available <http://hdl.handle.net/2318/1648503> since 2017-10-02T12:35:13Z

Published version:

DOI:10.1007/s00429-016-1361-3

Terms of use:

Open Access

Anyone can freely access the full text of works made available as "Open Access". Works made available under a Creative Commons license can be used according to the terms and conditions of said license. Use of all other works requires consent of the right holder (author or publisher) if not exempted from copyright protection by the applicable law.

(Article begins on next page)

This is the author's final version of the contribution published as:

Parolisi R., Cozzi B., Bonfanti L.

Non-neurogenic SVZ-like niche in dolphins, mammals devoid of olfaction

BRAIN STRUCTURE AND FUNCTION

2017 Aug;222(6):2625-2639 Epub 25 feb 2017

The publisher's version is available at:

10.1007/s00429-016-1361-3

When citing, please refer to the published version.

Link to this full text:

<http://hdl.handle.net/2318/1648503>

This full text was downloaded from iris-AperTO: <https://iris.unito.it/>

1 **Non-neurogenic SVZ-like niche in dolphins,**
2 **mammals devoid of olfaction**

3
4 Parolisi R.^{1,2}, Cozzi B.³, Bonfanti L.^{1,2*}
5

6 ¹ Neuroscience Institute Cavalieri Ottolenghi (NICO), Orbassano, Italy; ² Department of Veterinary
7 Sciences, University of Turin, Torino, Italy; ³ Department of Comparative Biomedicine and Food
8 Science, University of Padua, Legnaro, Italy.
9

10
11 Abbreviated title: Absence of adult neurogenesis in dolphins
12

13 Number of figures, tables: 7 Figures, 4 Tables
14

15
16 * Correspondence to:
17

18 Luca Bonfanti, DVM, PhD
19 Department of Veterinary Sciences
20 Via Leonardo da Vinci, 44
21 10095 Grugliasco (TO)
22 University of Turin, Italy
23 Email: luca.bonfanti@unito.it
24
25

26
27 Keywords: adult neurogenesis, olfactory bulb, cetaceans, subventricular zone, brain plasticity,
28 evolution, doublecortin
29

30 **Abstract**

31 Adult neurogenesis has been implicated in brain plasticity and brain repair. In mammals, it is
32 mostly restricted to specific brain regions and specific physiological functions. The function and
33 evolutionary history of mammalian adult neurogenesis has been elusive so far. The largest
34 neurogenic site in mammals (subventricular zone, SVZ) generates neurons destined to populate the
35 olfactory bulb. The SVZ neurogenic activity appears to be related to the dependence of the species
36 on olfaction since it occurs at high rates throughout life in animals strongly dependent on this
37 function for their survival. Indeed, it dramatically decreases in humans, who do not depend so much
38 on it. This study investigates whether the SVZ neurogenic site exists in mammals devoid of
39 olfaction and olfactory brain structures, such as dolphins. Our results demonstrate that a small SVZ-
40 like region persists in these aquatic mammals. However, this region seems to have lost its
41 neurogenic capabilities since neonatal stages. In addition, instead of the typical newly generated
42 neuroblasts, some mature neurons were observed in the dolphin SVZ. Since cetaceans evolved from
43 terrestrial ancestors, non-neurogenic SVZ may indicate extinction of adult neurogenesis in the
44 absence of olfactory function, with the retention of an SVZ-like anatomical region either vestigial
45 or of still unknown role.

46

47

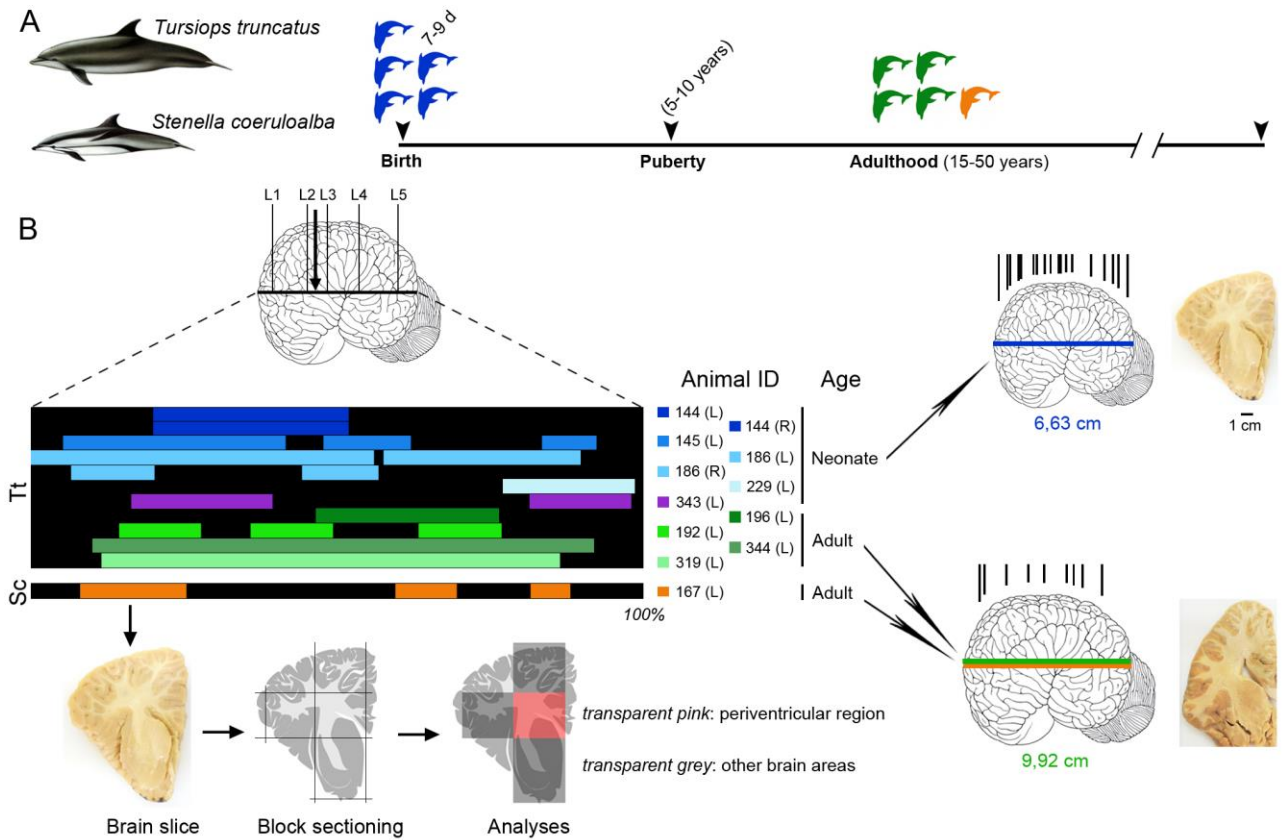
48 **Introduction**

49 Adult neurogenesis is a widely-conserved feature in vertebrates, generally undergoing
50 'phylogenetic reduction' from amphibians to humans within tetrapods (Kempermann, 2012;
51 Grandel and Brand, 2013). Despite remarkable discoveries leading to a better understanding of this
52 process, the underlying logic of adult neurogenesis in evolution, as well as its function, are still a
53 matter of debate. In all mammals studied so far, lifelong neurogenesis persists within two canonical
54 neurogenic sites (Feliciano et al., 2015) or stem cell niches: the subventricular zone located in the
55 forebrain (SVZ; Tong and Alvarez-Buylla, 2014) and the subgranular zone of the dentate gyrus in
56 the hippocampus (SGZ; Vadoaria and Gage, 2014). The production of new neurons acts as a sort of
57 'metaplasticity' (second-level plasticity) primarily linked to learning tasks performed within specific
58 neural systems, such as olfactory learning within the olfactory bulb (Lepousez et al., 2013;
59 Sakamoto et al., 2014) in addition to memory and pattern separation in the hippocampus (Aimone et
60 al., 2014; Sahay et al., 2011). However, the ultimate function/aim of adult neurogenesis as a
61 conserved biological process is far from being identified. Substantial differences exist in the
62 extension and importance of neurogenic sites with respect to species, age, brain region and
63 ecological niche, thus making it difficult to identify any common traits (Barker et al., 2011;
64 Bonfanti and Peretto, 2011; Sanai et al., 2011; Amrein, 2015; Kempermann, 2016).

65 In terrestrial mammals, the SVZ is the largest neurogenic site (Bordiuk et al., 2014) which provides
66 new neurons for the olfactory bulb through the rostral migratory stream (Lois and Alvarez-Buylla,
67 1994). The SVZ neurogenic activity appears related to the importance of olfaction, since it occurs at
68 high rates throughout life in animals strongly dependent on olfactory functions for their survival
69 (e.g., rodents; Lepousez et al., 2013). Whereas in humans, who have smaller olfactory bulbs and do
70 not depend so much on olfaction the production of new neurons dramatically decreases with age
71 (Sanai et al., 2011). Apart from the lack of a deeper understanding of this trend, it is still unknown
72 whether the existence of adult SVZ neurogenesis is actually dependent on olfactory functions and

73 related brain structures. Additionally, the search for the answer to the pivotal question of the
74 evolutionary interpretation of the functions of neurogenesis during the tetrapod evolution still
75 remains unanswered. Hence, in this study we investigated whether the forebrain neurogenic niche is
76 present in natural animal models devoid of olfaction, namely, the dolphins. Marine Cetartiodactyla
77 live underwater and have developed alternative techniques for navigation, foraging and tracking of
78 prey (echolocation; Marriott et al., 2013). Thus, unlike terrestrial mammals and fish, they possess
79 significantly reduced or absent olfactory systems (Breathnach, 1953; Breathnach and Goldby, 1954;
80 Oelschläger, 2008). Even within other adult cetaceans, such as mysticetes, which possess a reduced
81 olfactory system (Oelschläger and Oelschläger, 2009), dolphins have completely lost olfaction
82 (Oelschläger, 2008; Cozzi et al., 2017). The terminal nerve is the only surviving component of the
83 three functional systems, namely, the olfactory, vomeronasal, terminal systems in the nasal region
84 of the mammalian's head (Ridgway et al., 1987). A recent report (Parolisi et al., 2015),
85 demonstrated that neonatal dolphins lack the thick SVZ germinative layer typically persisting at
86 birth on the ventricle wall of terrestrial mammals (Tramontin et al., 2003; Peretto et al., 2005),
87 including humans (Del Bigio, 2011; Sanai et al., 2011). This finding might be due to either the
88 advanced developmental stage of the dolphin brain at birth (Ridgway, 1990) or the absence of
89 olfaction, with the possibility that periventricular neurogenesis could be absent in these aquatic
90 mammals since birth. In addition, a recent study showed that several cetacean species have small
91 hippocampi which do not stain for doublecortin (Patzke et al., 2015), thus indicating the possibility
92 that adult neurogenesis itself might be lacking in these animals. Nevertheless, due to their large
93 brain size and scarce availability of tissues that are fixed well (dolphins are legally protected
94 animals on the basis of ethical and environmental issues), current knowledge by no means excludes
95 the existence of postnatal neurogenesis in these animals. In the present study, the periventricular
96 region of ten dolphins belonging to two different species (*Tursiops truncatus*, bottlenose dolphin;
97 *Stenella coeruleoalba*, striped dolphin; Fig. 1 and Table 1) and ages (neonatal and adult) were

98 carefully analyzed using histology and immunocytochemistry in order to investigate the presence
 99 (or absence) of a neurogenic SVZ similar to terrestrial mammals.



100

101 Fig 1

102 **Materials and methods**

103

104 **Tissue samples**

105 *Dolphin tissues*

106 In this study we used brain samples obtained from 10 dolphins, 9 bottlenose dolphins (*Tursiops*
 107 *truncatus* Montagu, 1821 - *T. truncatus*) and 1 striped dolphin (*Stenella coeruleoalba* Meyen, 1833
 108 - *S. coeruleoalba*) stored in the Mediterranean Marine Mammal Tissue Bank (MMMTB) of the
 109 University of Padova at Legnaro, Italy (see Table 1 and Fig. 1). The MMMTB is a CITES
 110 recognized (IT020) research center and tissue bank, sponsored by the Italian Ministry of the
 111 Environment and the University of Padova, with the aim of harvesting tissues from wild and captive

112 cetaceans and distributing them to qualified research centers worldwide. The bottlenose and the
113 striped dolphins have a very similar shape and anatomy. Although, differences in size and weight
114 are evident in oceanic animals, (*T. truncatus* is generally larger than *S. coeruleoalba*) they are
115 reduced in dolphins that live in relatively smaller basins (including the Mediterranean Sea).

116 Tissue samples consisted of brain coronal slices (see Parolisi et al., 2015, Morgane et al., 1980, and
117 Fig. 1) approximately 1-1,5 cm thick, collected during post-mortem procedures performed in the
118 necropsy room of the Department of Comparative Biomedicine and Food Science of the University
119 of Padova at Legnaro, and fixed by immersion in 4% buffered formalin. Post-mortem delay before
120 actual sampling varied between a minimum of 18 to a maximum of 40 hours.

121 To confirm the immunodetection of Ki-67 antigen within an active germinal layer and to quantify
122 its cell proliferation density, we sampled tissue blocks from the top of the left cerebellar hemisphere
123 from neonatal dolphins to investigate the immunodetection of Ki-67 antigen within an active
124 germinal layer and to quantify its cell proliferation density (see Parolisi et al., 2015).

125

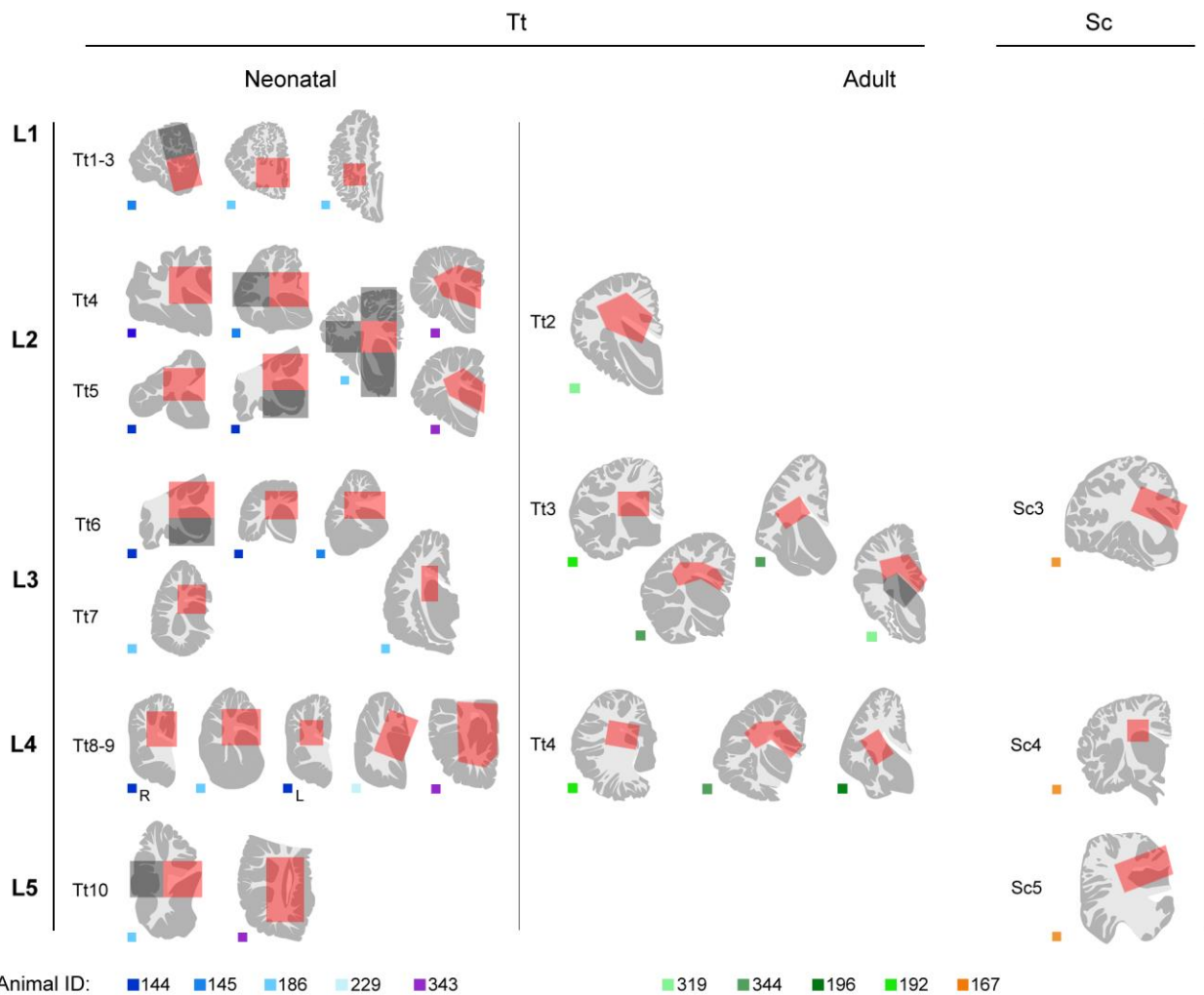
126 **Gross anatomy of the dolphin tissue slices**

127 To obtain a representation of single brain levels, the anterior face of thick brain slices was
128 photographed and imported on Neurolucida (Micro-Brightfield, Colchester,VT). Here, the outlines
129 of each coronal section, including those of the external (pial) surface and those at the white
130 matter/grey matter limits, were drawn (Fig. 1B). The contours were then imported to Photoshop to
131 obtain images of each brain level. The whole procedure has been described previously in detail
132 (Parolisi et al., 2015).

133

134 **Tissue processing for histology and immunocytochemistry**

135 Smaller blocks were cut from thick, formalin-fixed tissue slices (about 1,5x2,5 cm; see Fig. 1 and
 136 Parolisi et al., 2015), washed in 0.1M phosphate buffer (PB), pH 7.4, for 24 hours, then
 137 cryoprotected in graded concentrations of sucrose solutions up to 30% in 0.1M PB and
 138 subsequently frozen by immersion in liquid nitrogen-chilled isopentane at -80°C. Cryostat sections
 139 (40 µm thick) were cut on glass slides treated with 3-Aminopropyltriethoxysilane (Sigma-Aldrich,
 140 741442) and processed for histological and immunocytochemical analyses. All thick slices and
 141 relative blocks used in this study at different anterior-posterior brain levels and ages are
 142 summarized in Fig. 2.



143

144 Fig. 2

145 For immunocytochemical analysis, two different protocols of indirect staining were employed
 146 namely, the peroxidase or the immunofluorescence techniques. In peroxidase protocol, the sections

147 were pre-incubated in 1% H₂O₂ - phosphate saline buffer (PBS) for 20 min, rinsed in PBS and then
148 pre-incubated in blocking buffer (3% horse serum (HS), 2% bovine serum albumin (BSA), 1%
149 Triton X-100 in 0.01 M PBS, pH 7.4) for 1h at room temperature to reduce non-specific staining.
150 Then the sections were incubated for 24–48 h at 4°C in a solution of 0.01M PBS, pH 7.4,
151 containing 0.5% Triton X-100, 2% HS, 1% BSA and the primary antibody. Immunohistochemical
152 reactions were performed by the avidin–biotin–peroxidase method (Vectastain ABC Elite kit;
153 Vector Laboratories, Burlingame, CA, USA) and revealed using 3,3'-diaminobenzidine (3% in Tris-
154 HCl) as chromogen. Sections were counterstained with Cresyl violet staining, according to standard
155 procedures described previously (see Ponti et al. 2006a,b), mounted with DPX Mountant (Sigma-
156 Aldrich, 06522) and examined using an E-800 Nikon microscope (Nikon, Melville, NY) connected
157 to a colour CCD Camera. In immunofluorescence staining the sections were rinsed in PBS and then
158 pre-incubated in blocking buffer (3% horse serum (HS), 2% bovine serum albumin (BSA), 1-2%
159 Triton X-100 in 0.01 M PBS, pH 7.4), for 1h at room temperature. Then the sections were incubated
160 for 24–48 h at 4°C in a solution of 0.01M PBS, pH 7.4, containing 1-0.5% Triton X-100, 2% serum,
161 1% BSA and the primary antibody. Following primary antisera incubation, sections were incubated
162 with appropriate solutions of secondary cyanine 3 (Cy3)-conjugated (1:800; Jackson
163 ImmunoResearch, West Grove, PA) and Alexa 488-conjugated (1:800; Molecular Probes, Eugene,
164 OR) antibodies, for 2 hours RT. Sections were counterstained with 4',6-diamidino-2-phenylindole
165 (DAPI, KPL, Gaithersburg, Maryland USA), mounted with MOWIOL 4-88 (Calbiochem, Lajolla,
166 CA). The antibodies and the dilutions used were as follows: doublecortin (DCX), polyclonal,
167 rabbit, AbCam, 1:1000-1:1800, and polyclonal goat, Santa Cruz, 1:700; GFAP, polyclonal, rabbit,
168 Dako, 1:2000; Ki-67 antigen, polyclonal, rabbit, Novocastra, 1:600-1:1000; vimentin (VIM),
169 monoclonal, mouse (40EC), Exbio, 1:800; calretinin (CR), polyclonal, rabbit, Santa Cruz, 1:200,
170 and MAP2, monoclonal, mouse, Millipore, 1:1000 (a list of antibodies tested in this study that
171 failed to demonstrate immunostating on the dolphin tissues in the present study is provided in Table
172 2). To reveal the immunohistochemical and immunofluorescence reactions, the sections were

173 examined using an E-800 Nikon microscope (Nikon, Melville, NY) connected to a colour CCD
174 Camera, a Leica TCS SP5 (Leica Microsystems, Wetzlar, Germany) confocal microscope, and a
175 Nikon Eclipse 90i. (Nikon, Melville, NY) confocal microscope.

176

177 **Image processing and data analysis**

178 All images were processed using Adobe Photoshop CS4 (Adobe Systems, San Jose, CA). Only
179 general adjustments to color, contrast, and brightness were made. Quantitative evaluations were
180 performed through the Neurolucida software (MicroBrightfield, Colchester, VT). The parameters
181 considered were as follows: Ki-67+ cell density in SVZ-lr, ScWM, and corpus callosum (18
182 sections for neonates, 7 sections for subadult, 60 sections for adults), and in EGL (20 sections/ages);
183 distance between lateral ventricle wall and SVZ-lr (three measures performed on 33 sections for
184 neonates and 12 sections for adults); evaluation of the continuous gap between SVZ-lr and ScWM
185 cell clusters (31 sections in neonates, at L3). The averages measured of the cell body diameter of
186 SVZ-lr tightly-packed cells (20 cells) and SVZ-lr neurons (20 cells), diameter of ScWM cell
187 clusters (181 clusters), Cm (27 measurements) and Cms areas (69 measurements) did not deviate
188 significantly from normal distribution (Shapiro Wilk test for data $n < 30$; Anderson-Darling test for
189 $n > 30$).

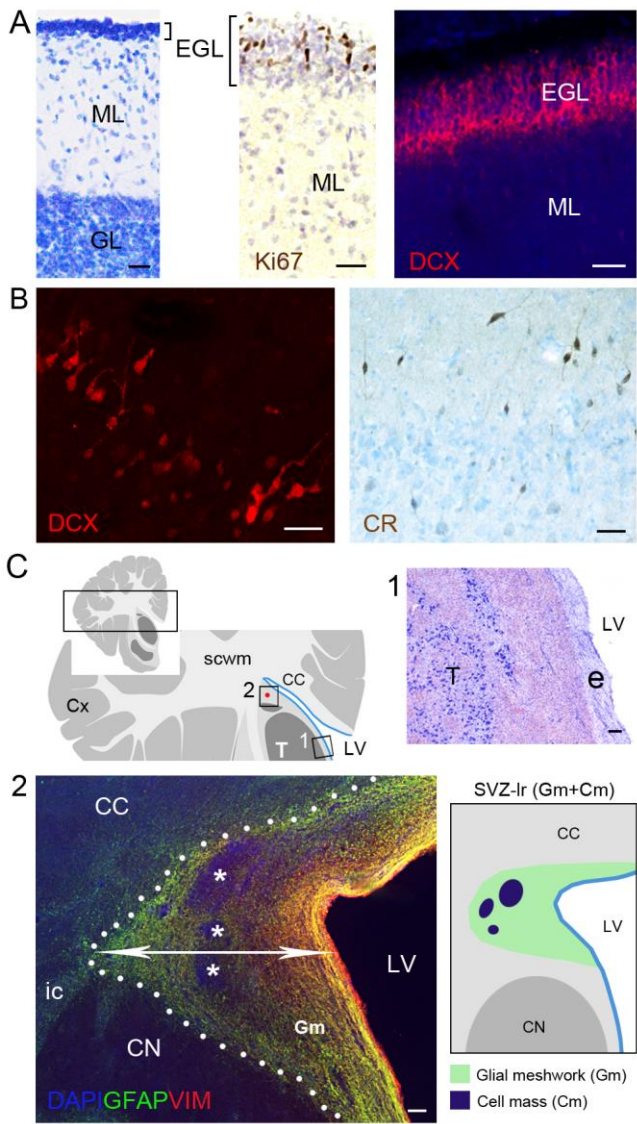
190 All the graphs were constructed using Graph Pad Prism (San Diego California, USA). Statistical
191 analyses were performed by Graph Pad Prism software and included unpaired (two-tailed) Student's
192 t test (comparing only two groups). $p < 0.05$ was considered as statistically significant. Data are
193 expressed as averages \pm standard deviation (SD).

194

195

196 **Results**

197 Considering the remarkable size of the adult dolphin brain (about 10 cm length and 1,3-1,7 Kg
198 weight, in adult *T. truncatus*), and the understanding that SVZ neurogenesis is most prominent at
199 birth in terrestrial mammals, we began the analyses on neonates, using the atlas of the
200 neonatal/early postnatal dolphin forebrain as an anatomical reference (Parolisi et al., 2015). Careful
201 histological screening and immunocytochemical analyses were carried out on the entire
202 periventricular region (Fig. 2 and Table 3) in search for signs of any remnants resembling a typical
203 neurogenic niche. Staining specificity for the cytoskeletal protein doublecortin (DCX; consistently
204 expressed in newly generated neuroblasts and immature neurons; Nacher et al., 2001; Brown et al.,
205 2003) and the marker for cell proliferation, namely the Ki-67 antigen (Kee et al., 2002) was
206 confirmed by immunocytochemical detection of granule cell precursors in the external germinal
207 layer (EGL) of the neonatal dolphin cerebellar cortex, which served as internal control (Fig. 3A).
208 DCX staining was further tested in neonatal and adult dolphin brains by detection of a population of
209 immature neurons occurring in the superficial layers of the cerebral cortex of most mammals
210 studied so far (references in Bonfanti and Nacher, 2012; Fig. 3B).



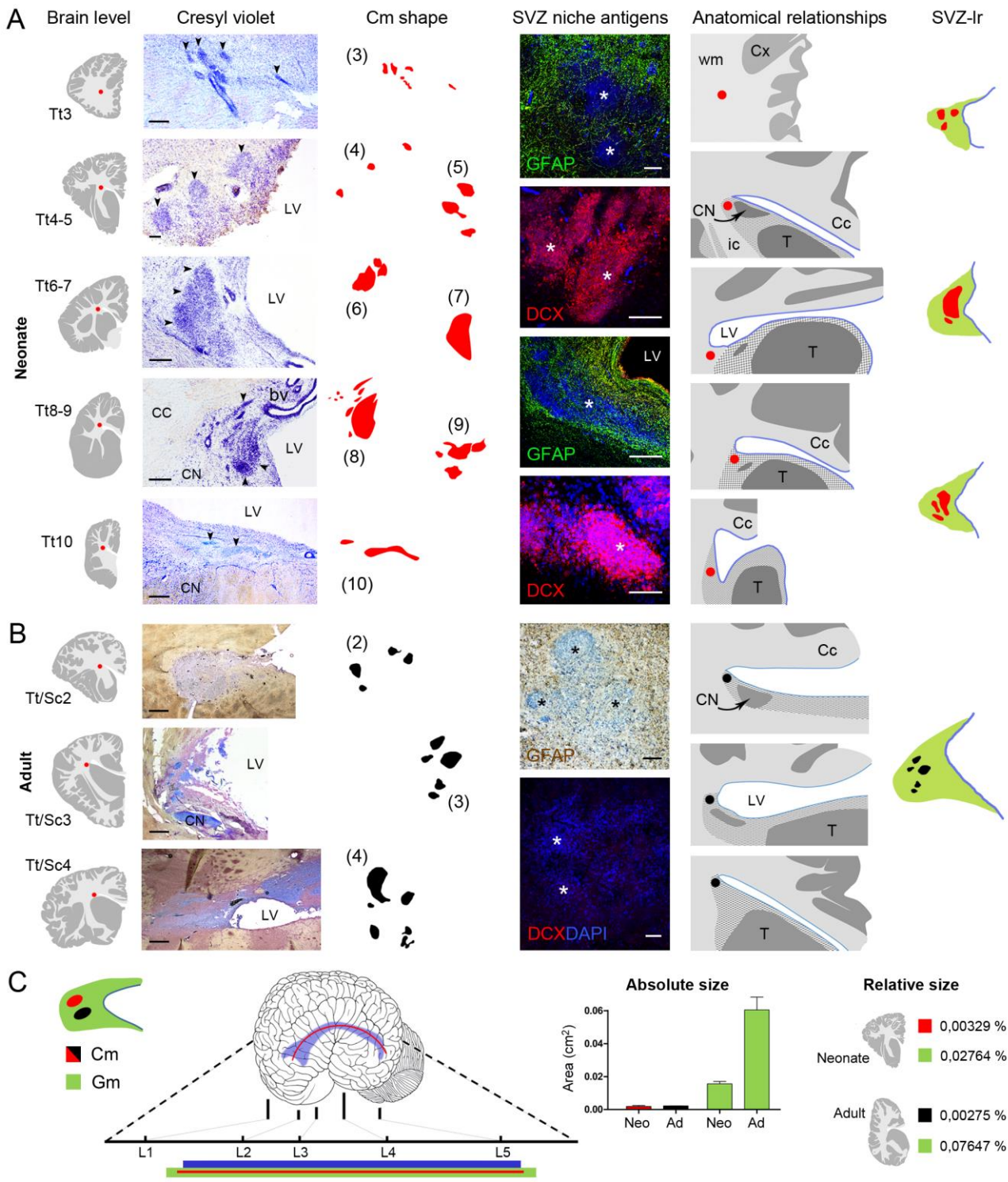
211

212 Fig 3

213 **Identification of a SVZ-like region in neonatal and adult dolphins**

214 Histological screening in the brain periventricular region of neonatal *T. truncatus* confirmed the
 215 absence of a well recognizable sub-ependymal germinal layer along most of the lateral ventricle
 216 wall (Parolisi et al., 2015; Fig. 3C1), yet clusters of small tightly-packed cells (3,4-0,63 μm - cell
 217 body diameter) were detected in a restricted region located at its dorsolateral corner, from level Tt3
 218 to Tt10 (Figs. 3C2 and 4). Systematic analysis carried out on serial sections (see Table 3 for
 219 anteroposterior brain level steps) revealed that these clusters form a very thin, continuous cell mass

220 (Cm; $145615,06 \pm 68402,16 \mu\text{m}^2$ - average area at L2-L4 levels; see Table 4) lining the entire lateral
221 ventricle extension and reaching a length of approximately 4,9 cm (estimated by considering
222 consecutive brain sections cut following the beak-fluke axis that contained the Cm; see Morgane et
223 al., 1980 and Fig. 4). Immunocytochemical detection of the astrocyte marker glial fibrillary acidic
224 protein (GFAP) revealed a dense glial meshwork (Gm) completely surrounding the Cm, sharply
225 ending at the limit with the corpus callosum (dorsal and lateral) and the forebrain caudate nucleus
226 (lateral and ventral; Figs. 3 and 4). The Cm was never observed to be directly in contact with the
227 ventricular wall, maintaining an evident distance from the ependyma (Fig. 4 and below). At the
228 most anteroposterior brain levels, the Cm was split in smaller cell clusters (Cms; $6210,76 \pm 3866,14$
229 μm^2 - average area at L1 and L5 levels), their number varying from 1 to 12, being higher at the
230 extremities and lower in the middle (Fig. 4 and Table 4). The neuroblast-like nature of these cells
231 was suggested by their DCX expression (Fig. 4A). On the whole, this region appears to be
232 organized into two main cellular compartments (Cm and Gm) that seem phylogenetically related to
233 the adult SVZ described in most terrestrial mammals (Lois et al., 1996; Peretto et al., 1997,2005;
234 Bonfanti and Peretto, 2011), and thus referred hereafter to as SVZ-like region (SVZ-lr).



235

236 Fig 4

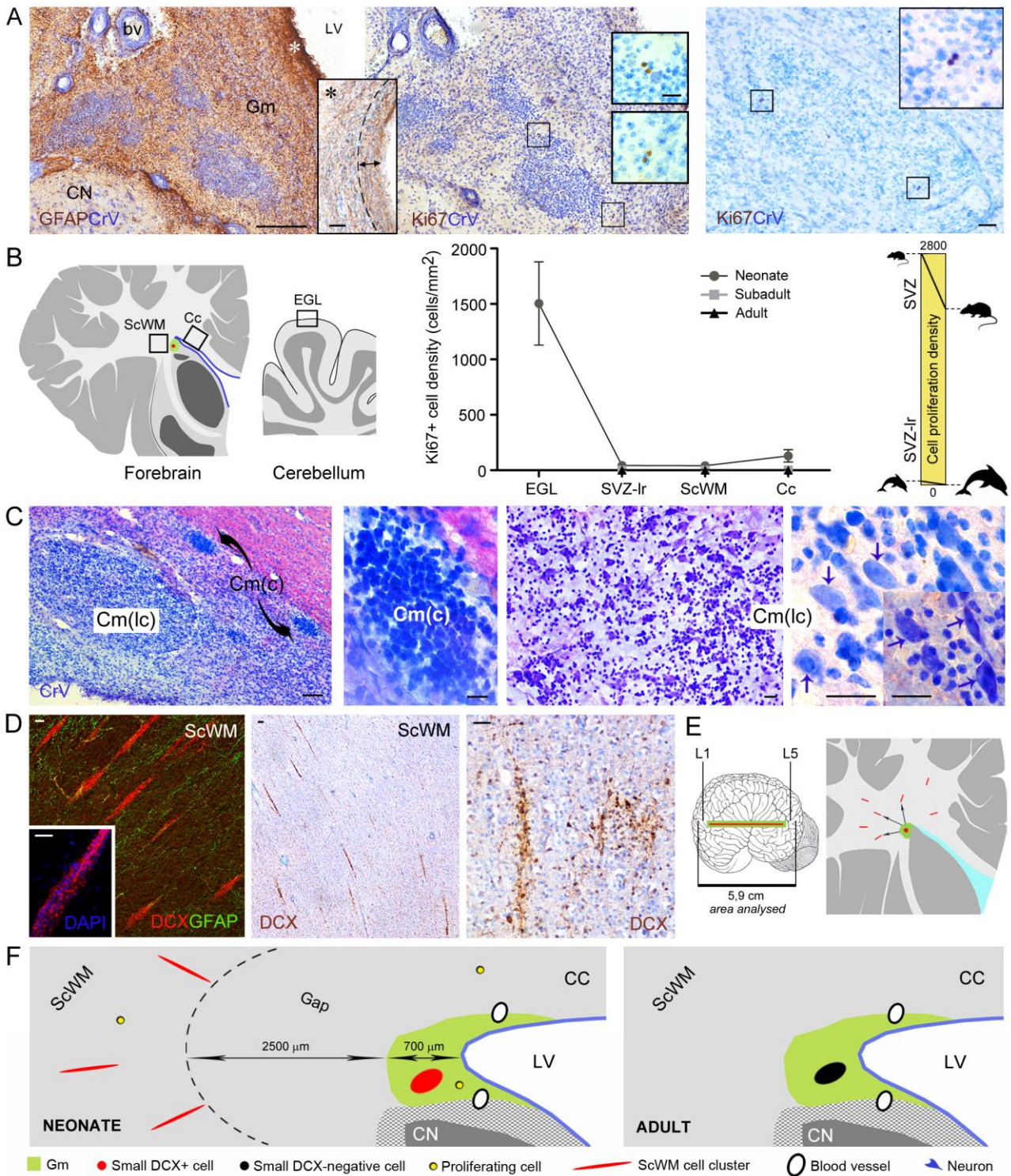
237 An SVZ-Ir similar to that of neonates, sharing the same location, was identified in adult dolphins
 238 belonging to both species (Fig. 4B). Analysis of the SVZ-Ir total area and Cms area in neonatal and
 239 adult brains revealed a slight increase in size for the SVZ-Ir in adults with respect to neonates,
 240 whereas no major changes were observed in the Cm size through ages (Fig. 4C and Table 4).

241

242

243 **Periventricular neurogenic processes in dolphins are almost exhausted at birth and absent in**
244 **adulthood**

245 Immunocytochemical detection of Ki-67 antigen revealed only a few scattered proliferating cells in
246 the whole SVZ-lr of neonatal animals (Fig. 5A) and none in adults. In the neonatal SVZ-lr the Ki-
247 67+ nuclei appeared evenly distributed both in Cm and Gm, their frequent appearance in doublets
248 indicative of the absence of cell migration. Quantitative analysis revealed very low rates of cell
249 proliferation (average cell density/mm² 43,16±32,92; Table 4) substantially similar to those in the
250 surrounding parenchymal tissue (Fig. 5B). In the young *T. truncatus* (subadult), such rate was even
251 lower than in the corpus callosum (Fig. 5B and Table 4) wherein a low, protracted proliferation of
252 glial cell precursors is known to occur (Dawson et al., 2003). The number of proliferating cells in
253 the neonatal dolphin SVZ-lr was found to be negligible when compared with those typically found
254 in the correspondent neurogenic site of terrestrial mammals (average cell density/mm² 2657±86, see
255 Armentano et al., 2011 and Fig. 5B, right). This is possibly indicative of the precocious exhaustion
256 of neurogenic activity at birth.

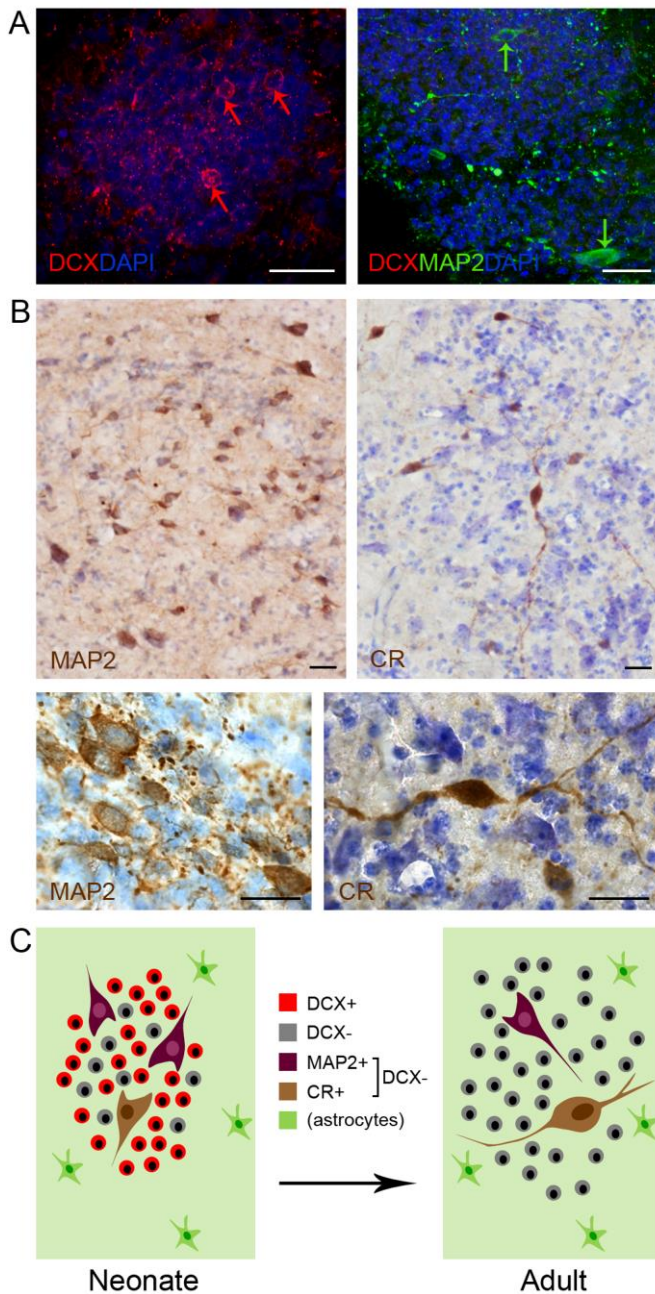


257

258 Fig 5

259 Other features previously unnoticed in terrestrial mammals were also observed in the internal
 260 organization of the Cms. Some of the cell clusters appeared "less compact", with small-sized cells
 261 more sparse and distant to each other (Fig. 5C). In the neonatal SVZ-lr, many of these cells were
 262 not expressing DCX (Fig. 6A) and were intermingled with larger cells morphologically

263 recognizable as neurons with triangular- or bipolar-shaped soma ($5,74 \pm 1,36 \mu\text{m}$ - cell body
264 diameter; Fig. 5C). Most of these cells were immunoreactive for the neuronal marker microtubule-
265 associated protein 2 (MAP2; Herzog and Weber, 1978; Fig. 6), whereas, a smaller population
266 (around 15-30% - value estimated on 5 sections for each age performed at the L3-L4 levels)
267 expressed the calcium-binding protein calretinin (CR; von Bohlen and Halbach, 2011; Fig. 6; see
268 Fig. 3B for internal control). The partial lack of DCX staining, along with the expression of
269 neuronal maturation markers, strongly confirm a progressive loss of neurogenic activity in the
270 dolphin SVZ-lr starting at very early ages. Similarly, no DCX staining was detectable in the SVZ-lr
271 of adult dolphins (Fig. 4B and 6A), wherein the CR⁺ neurons showed further signs of
272 differentiation, i.e. the extension of neuritic processes (Fig. 6).



273

274 Fig 6

275 SVZ neurogenesis provides neuronal precursors for the olfactory bulb in all terrestrial mammals
 276 (Lois and Alvarez-Buylla 1994; Bonfanti and Ponti, 2008). Thus, the occurrence of an SVZ-lr in the
 277 brains of aquatic mammals raises the question as to whether some streams do exist in spite of the
 278 absence of olfaction/olfactory bulb in these animals. To answer this question, the subcortical white
 279 matter (ScWM) surrounding the entire SVZ-lr was analyzed at all ages in search for DCX+
 280 cells/streams. In the neonates, elongated clusters of small, tightly-packed cells were detectable (Fig.
 281 5D). Both compact, thick and less compact, thin clusters ($37,52 \pm 35,47 \mu\text{m}$ - transverse diameter,

282 with substantial variability in different animals) were observed (Fig. 5D). They were mostly
283 radially-oriented in large portions of the ScWM, occupying a fan-shaped area along the inner part of
284 the hemisphere (anteriorly, laterally, ventrally, and posteriorly to the SVZ-lr), yet never reaching the
285 cortex. Since the shape of these structures might be somehow reminiscent of the "parenchymal
286 chains" of neuroblasts previously described in other mammals (Luzzati et al., 2003; Ponti et al.,
287 2006a), they were investigated for possible presence of dividing cells and/or connection with the
288 SVZ-lr and its Cms. No Ki-67+ cells were ever detectable in association with the ScWM cell
289 clusters, although a few proliferating cells were occasionally found in the tissue among the clusters
290 (Fig. 5F). Upon careful analysis carried out all along the SVZ-lr (see Fig. 5E and Table 3 for serial
291 section steps), it was found that no direct connections ever occurred between the SVZ-lr and any of
292 the ScWM cell clusters. Rather, a continuous "gap" completely devoid of cell clusters (2500 ± 200
293 μm thick; Fig. 5E,F) was present in the areas surrounding the SVZ-lr, in every direction, including
294 anterior and posterior aspects, thus excluding the possibility that they are continuous streams of
295 cells generated within the SVZ-lr.

296

297

298

299 **Discussion**

300

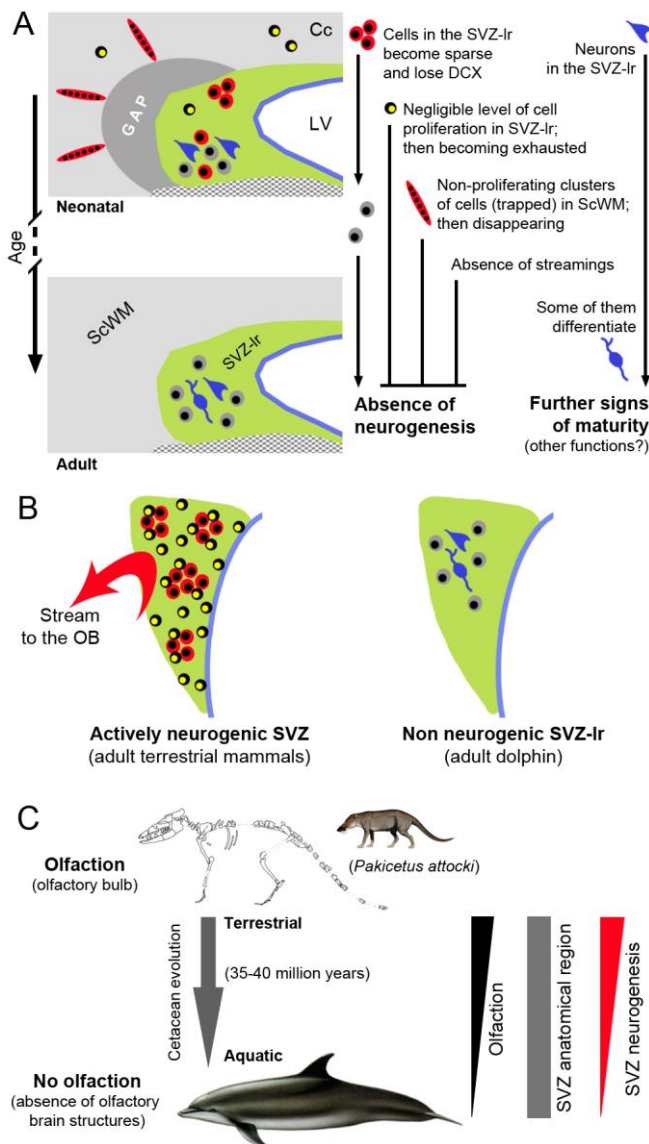
301 The brains of all terrestrial mammals host a remnant of the periventricular, embryonic germinal
302 layer (SVZ) particularly prominent at birth (Tramontin et al., 2003; Peretto et al., 2005) and
303 persisting throughout life as a major neurogenic site (Kriegstein and Alvarez-Buylla, 2009; Bordiuk
304 et al., 2014). Here we show that dolphins, although lacking such a layer, host a very small SVZ-lr
305 located at a remote tip of the lateral ventricle, which can be consistently found at neonatal and adult
306 ages. The SVZ-lr occupies an area approximately similar the real size of its counterpart in mice

307 (Fig. 4C), whose brain, in comparison, is 40 fold smaller if a correspondent coronal section area is
308 measured, and 3000 fold smaller if the weight or volume are considered (Rose et al., 2006; Marino
309 et al., 2000).

310 Unlike the SVZ of terrestrial mammals (Tramontin et al., 2003; Lois et al., 1996; Peretto et al.,
311 1997,2005), the SVZ-lr of dolphins is already compartmentalized soon after birth with its structure
312 being reminiscent of adult neurogenic sites (Ponti et al., 2006a; Bonfanti and Ponti, 2008). This
313 phenomenon, although unusual in mammals, fits well with the highly advanced developmental
314 stage of the brain in neonatal aquatic mammals (Parolisi et al., 2015), which is related to the
315 immediate need of the newborn to already possess all the swimming competences required for life,
316 including the ability to reach the surface and breathe (Ridgway, 1990). Yet, it is surprising that a
317 brain region sharing features (location, inner histological organization and some molecular aspects)
318 with the SVZ neurogenic niche of terrestrial mammals does persist in dolphins, apparently in
319 contrast with the absence of olfaction/olfactory structures. What appears to be unique in this SVZ-lr
320 is its extremely low rate of cell proliferation detectable in neonates, followed by utter
321 disappearance. The density of dividing cells revealed by Ki-67 antigen localization in the SVZ-lr of
322 the neonatal dolphins ($43,16 \pm 32,92$) is 34 fold lower when compared with the germinal layer of the
323 cerebellar cortex in the same animals ($1504,63 \pm 374$; Figs. 3 and 5 and Table 4), 62 fold lower than
324 that existing in the SVZ of neonatal rodents (2657 ± 86 ; Armentano et al., 2011), 47 fold lower than
325 in adult rodents ($2018,5 \pm 420$; Rolando et al., 2012; Fig. 5), and it is not higher than in the
326 surrounding brain parenchyma (Fig. 5B). Even in humans, despite a dramatic reduction of SVZ
327 thickness with age (Sanai et al., 2011), a highly proliferative region exists in neonates, which
328 persists to a lesser extent in adult and old individuals (Eriksson et al., 1998; Sanai et al., 2004;
329 Wang et al., 2011).

330 The very early exhaustion of peri-ventricular neurogenic activity in dolphins is also reflected by the
331 cellular and molecular features of the Cms in the SVZ-lr. In neonates, the small, neuroblast-like

332 cells are not tightly-packed, show variable and incomplete DCX staining and are intermingled with
 333 neurons expressing mature neuronal markers such as MAP2 and CR (Figs. 5-7).



334

335 Fig 7

336 In adults, no DCX staining is detectable, whereas the SVZ-ir neurons are still detectable, a
 337 subpopulation of them showing further traits of differentiation such as the extension of neuritic
 338 processes (Fig. 6). Hence, in the dolphin SVZ-ir an early exhaustion of cell division goes in parallel
 339 with neuronal maturation. Such differentiation "in situ" might simply be a consequence of the
 340 cellular/molecular environment of the SVZ-ir (e.g., absence of any continuous supply of new,
 341 young neuroblasts) which is no more supportive as an active stem cell niche. These observations are
 342 in sharp contrast with the current knowledge on the SVZ of all terrestrial mammals, characterized

343 by an embryonic-like tissue which persists into adulthood (Fig. 7), although with different degrees
344 of proliferative activity from rodents to humans (Ponti et al., 2013; Eriksson et al., 1998; Wang et
345 al., 2011; Sanai et al., 2004,2011). Additionally, a careful analysis extended to the brain regions
346 surrounding the SVZ-lr did not reveal any streams of cells spanning from the periventricular Cms to
347 any other direction, unlike terrestrial mammals which all exhibit a marked rostral migratory stream
348 at perinatal stages (Lois and Alvarez-Buylla 1994; Peretto et al., 2005). Although the radially-
349 oriented, DCX+ cell clusters present in the ScWM of neonates were reminiscent of "chain-like"
350 structures (Luzzati et al., 2003; Ponti et al., 2006a), the occurrence of a continuous white matter gap
351 (absence of any direct contact with the SVZ-lr perimeter) along with the scarcity of cell divisions in
352 the SVZ-lr itself, exclude the possibility that they can represent any product of an ongoing
353 neurogenic activity.

354 Once it is established that in dolphins all SVZ neurogenic processes are substantially exhausted at
355 birth, clusters of DCX+ cells still present in the SVZ-lr and white matter of neonatal animals are a
356 matter of further investigation. The occurrence of DCX+ cells in the periventricular white matter or
357 in the corpus callosum has been previously shown in, large-brained mammals at postnatal ages
358 (Fung et al., 2011). Although DCX is commonly expressed in newly generated neuroblasts (Brown
359 et al., 2003), staining for this cytoskeletal protein alone is not at all a proof for the occurrence of
360 neurogenesis, since DCX is heavily present in non-newly generated adult cell populations (Gomez-
361 Climent et al., 2008; Luzzati et al., 2009; Bonfanti and Nacher, 2012). Considering the extremely
362 rapid developmental growth of the dolphin brain and its remarkably advanced stage of maturation at
363 birth (Ridgway, 1990; Parolisi et al., 2015) the ScWM cell clusters appear to be previously
364 migrating streams of cells "trapped" in the thick white matter which fills the central part of the
365 hemispheres, as sort of "remnants" of the last neurogenic wave. In fact, no more DCX+ cells are
366 detectable in the entire ScWM of adults.

367 In this study, morphological, antigenic, proliferative aspects converge to support the conclusion that
368 the dolphin SVZ-lr is a vestigial structure not behaving as an active neurogenic site since very early

369 postnatal stages (Fig. 7). This finding is consistent with previous studies that demonstrate that
370 several cetacean species have small hippocampi which do not stain for DCX (Patzke et al., 2015),
371 and strongly indicate that adult neurogenesis is totally lacking in dolphins. The two main findings
372 of this study that can have evolutionary considerations are: 1) the lack of clear signs of active
373 neurogenesis in aquatic mammals devoid of working olfaction/olfactory brain structures, and 2) the
374 counterintuitive existence of an SVZ-like region throughout their lifespan. The former observation
375 supports the occurrence of a strict relationship between adult SVZ neurogenesis and olfaction,
376 confirming the hypothesis that in mammals the production of highly specific populations of new
377 neurons is selectively destined for physiological roles such as learning, memory and plasticity
378 (Bonfanti, 2011; Peretto and Bonfanti, 2014; Obernier et al., 2014). On the other hand, the
379 persistence of an anatomical region reminiscent of the SVZ neurogenic niche (in fact, non-
380 neurogenic at all) plays against the simple hypothesis that a mammal lacking olfaction should not
381 possess an SVZ-like region. The explanation for this might be found in the evolutionary history of
382 these animals. Dolphins, and more in general cetaceans, evolved from terrestrial artiodactyls that
383 returned to the sea 35-40 million years ago (Thewissen et al., 2001). Data from fossil studies show
384 that the terrestrial ancestors of dolphins were wolf-sized terrestrial carnivorous (*Pakicetus*)
385 endowed with olfactory structures (Gingerich et al., 1983; Kishida et al., 2015). Then, in the early
386 Eocene period, by undergoing a gradual and branched transition from land to sea, they lost the
387 capacity to perceive odors (Gingerich et al., 1983; Thewissen et al., 2001). Although dolphin
388 fetuses possess small olfactory structures, they regress completely shortly after birth (Buhl and
389 Oelschläger, 1988; Cozzi et al., 2017). Adult dolphins only possess the terminal nerve, originating
390 from the olfactory placode and reaching the basal telencephalon (Buhl and Oelschläger, 1988).
391 While in adult terrestrial mammals, including man, the terminal system is reduced to a few hundred
392 neurons, in adult bottlenose dolphins (and other delphinid species), fiber strands and interspersed
393 ganglia enter the olfactory tubercle and the pre-piriform cortex (Ridgway et al., 1987). Yet, apart
394 from its common developmental origin with the olfactory system, the terminal nerve system is

395 completely independent from the SVZ germinal layer, both anatomically and functionally (Buhl and
396 Oelschläger, 1986).

397 Therefore, the retention of the SVZ-Ir in extant dolphins as an anatomical region having lost any
398 neurogenic capacity strongly suggests a slow extinction of adult neurogenesis in mammals not
399 dependent on olfaction for survival. The findings of the present study also open up the possibility
400 that non-neurogenic SVZ could have changed its role over time, from neurogenesis to new, yet
401 unknown roles. However, the latter aspect would hardly be an object of investigation in ethically
402 protected animals such as the toothed whales, unless new methods of analysis are developed in the
403 future.

404

405

406

407

408 **Acknowledgements:** the Authors thank Fondazione CRT for financial support (Bando Ricerca e
409 Istruzione 2014), the University of Turin (PhD programme in Veterinary Sciences), and the
410 MMTB of the University of Padova for supplying tissue samples of the dolphin brain. Special
411 thank to Antonella Peruffo, Mattia Panin, Stefano Montelli, Maristella Giurisato for their help in
412 gathering and handling the dolphin brain specimens, to Silvia Messina and Chiara La Rosa for
413 technical help in the cryostat sectioning, and to Telmo Pievani for reading the manuscript.

414

415

416

417

418

419

420 **References**

421

422 Aimone JB, Li Y, Lee SW, Clemenson GD, Deng W, Gage FH (2014) Regulation and function of
423 adult neurogenesis: from genes to cognition. *Physiol Rev* 94: 1991-1026.

424

425 Amrein I (2015) Adult hippocampal neurogenesis in natural populations of mammals. *Cold Spring*
426 *Harb Perspect Biol* 7(5) a021295.

427

428 Armentano M, Canalia N, Crociara P, Bonfanti L (2011) Culturing conditions affect viability and
429 organization of mouse subventricular zone in ex vivo cultured forebrain slices. *J Neurosci Meth*
430 197: 65-81.

431

432 Barker JM, Boonstra R, Wojtowicz JM (2011) From pattern to purpose: how comparative studies
433 contribute to understanding the function of adult neurogenesis. *Eur J Neurosci* 34: 963-977.

434

435 Bonfanti L (2011) From hydra regeneration to human brain structural plasticity: a long trip through
436 narrowing roads. *Sci World J* 11: 1270-1299.

437

438 Bonfanti L, Peretto P (2011) Adult neurogenesis in mammals - a theme with many variations. *Eur J*
439 *Neurosci* 34: 930-950.

440

441 Bonfanti L, Nacher J (2012) New scenarios for neuronal structural plasticity in non-neurogenic
442 brain parenchyma: the case of cortical layer II immature neurons. *Prog Neurobiol* 98: 1-15.

443

444 Bonfanti L, Ponti G (2008) Adult mammalian neurogenesis and the New Zealand white rabbit. *Vet*
445 *J* 175: 310-331.

446

447 Bordiuk OL, Smith K, Morin PJ, Semenov MV (2014) Cell proliferation and neurogenesis in adult
448 mouse brain. PLoS ONE 9(11): e111453.
449

450 Breathnach AS (1953) The olfactory tubercle, prepyriform cortex and precommisural region of the
451 porpoise (*Phocaenaphocaena*). J Anat 87: 96-113.
452

453 Breathnach A, Goldby F (1954) The amygdaloid nuclei, hippocampus and other parts of the
454 rhinencephalon in the porpoise (*Phocoenaphocoena*). J Anat 88: 267-291.
455

456 Brown JP, Couillard-Despres S, Cooper-Kuhn CM, Winkler J, Aigner L, Kuhn HG (2003)
457 Transient expression of doublecortin during adult neurogenesis. J Comp Neurol 467: 1-10.
458

459 Buhl EH, Oelschläger HA (1986) Ontogenetic development of the nervus terminalis in toothed
460 whales. Evidence for its non-olfactory nature. Anat Embryol 173: 285-294.
461

462 Buhl EH, Oelschläger HA (1988) Morphogenesis of the brain in the harbour porpoise. J Comp
463 Neurol 277: 109-125.
464

465 Cozzi B, Huggenberger S, Oelschläger HHA (2017) The anatomy of dolphins. Insights into body
466 structure and function. Chapter 6: Brain, Spinal Cord, and Cranial Nerves. Academic Press,
467 London, pp.191-285.
468

469 Dawson MRL, Polito A, Levine JM, Reynolds R (2003) NG2-expressing glial progenitor cells: an
470 abundant and widespread population of cycling cells in the adult rat CNS. Mol Cell Neurosci 24:
471 476-488.
472

473 Del Bigio MR (2011) Cell proliferation in human ganglionic eminence and suppression after
474 prematurity-associated haemorrhage. *Brain* 134, 1344-1361.

475

476 Eriksson PS, Perfilieva E, Bjork-Eriksson T, Alborn AM, Nordborg C, Peterson DA, Gage FH
477 (1998) Neurogenesis in the adult human hippocampus. *Nat Med* 4: 1313-1317.

478

479 Feliciano DM, Bordey A, Bonfanti L (2015) Noncanonical sites of adult neurogenesis in the
480 mammalian brain. *Cold Spring Harb Perspect Biol* 7(10):a018846.

481

482 Fung SJ, Joshi D, Allen KM, Sivagnanasundaram S, Rothmond DA, Saunders R, Noble PL,
483 Webster MJ, Weickert CS (2011) Developmental patterns of doublecortin expression and white
484 matter density in the postnatal primate prefrontal cortex and schizophrenia. *PLoS One* 6(9): e25194.

485

486 Gingerich PD, Wells NA, Russell DE, Shah SM (1983) Origin of whales in epicontinental remnant
487 seas: new evidence from the early eocene of pakistan. *Science* 220: 403-406.

488

489 Gomez-Climent MA, Castillo-Gomez E, Varea E, Guirado R, Blasco-Ibanez JM, Crespo C,
490 Martinez-Guijarro FJ, Nacher J (2008) A population of prenatally generated cells in the rat
491 paleocortex maintains an immature neuronal phenotype into adulthood. *Cereb Cortex* 18: 2229-
492 2240.

493

494 Grandel H, Brand M (2013) Comparative aspects of adult neural stem cell activity in vertebrates.
495 *Dev Genes Evol* 223: 131-147.

496

497 Herzog W, Weber K (1978) Fractionation of brain microtubule-associated proteins. Isolation of two
498 different proteins which stimulate tubulin polymerization in vitro. *Eur J Biochem* 92: 1-8.

499

500 Kee N, Sivalingam S, Boonstra R, Wojtowicz JM (2002) The utility of Ki-67 and BrdU as
501 proliferative markers of adult neurogenesis. *J Neurosci Meth* 115: 97-105.

502

503 Kempermann G (2012) New neurons for “survival of the fittest.” *Nat Rev Neurosci* 13: 727-736.

504

505 Kempermann G (2016) Adult neurogenesis: an evolutionary perspective. *Cold Spring Harb Perspect*
506 *Biol* 8:a018986.

507

508 Kishida T, Thewissen JGM, Hayakawa T, Imai H, Agata K (2015) Aquatic adaptation and the
509 evolution of smell and taste in whales. *Zool Lett* 1: 9.

510

511 Kriegstein A, Alvarez-Buylla A (2009) The glial nature of embryonic and adult neural stem cells.
512 *Annu Rev Neurosci* 32: 149-184.

513

514 Lepousez G, Valley MT, Lledo PM. (2013) The impact of adult neurogenesis on olfactory bulb
515 circuits and computations. *Annu Rev Physiol* 75: 339-363.

516

517 Lois C, Alvarez-Buylla A (1994) Long-distance neuronal migration in the adult mammalian brain.
518 *Science* 264: 1145-1148.

519

520 Lois C, Garcia-Verdugo JM, Alvarez-Buylla A (1996) Chain migration of neuronal precursors.
521 *Science* 271: 978-981.

522

523 Luzzati F, Peretto P, Aimar P, Ponti G, Fasolo A, Bonfanti L (2003) Glia-independent chains of
524 neuroblasts through the subcortical parenchyma of the adult rabbit brain. Proc Natl Acad Sci USA
525 100: 13036-13041.
526

527 Luzzati F, Bonfanti L, Fasolo A, Peretto P (2009) DCX and PSA-NCAM expression identifies a
528 population of neurons preferentially distributed in associative areas of different pallial derivatives
529 and vertebrate species. Cereb Cortex 19: 1028-1041.
530

531 Marino L, Rilling JK, Lin SK, Ridgway SH (2000) Relative volume of the cerebellum in dolphins
532 and comparison with anthropoid primates. Brain Behav Evol 56: 204-211.
533

534 Marriott S, Cowan E, Cohen J, Hallock RM (2013) Somatosensation, echolocation, and underwater
535 sniffing: adaptations allow mammals without traditional olfactory capabilities to forage for food
536 underwater. Zool Sci 30: 69-75.
537

538 Morgane PJ, Jacobs MS, McFarland WL (1980) The anatomy of the brain of the bottlenose dolphin
539 (*Tursiops truncatus*). Surface configurations of the telencephalon of the bottlenose dolphin with
540 comparative anatomical observations in four other cetaceans species. Brain Res Bull 5: 1-107.
541

542 Nacher J, Crespo C, McEwen BS (2001) Doublecortin expression in the adult rat telencephalon. Eur
543 J Neurosci 14: 629-644.
544

545 Obernier K, Tong CK, Alvarez-Buylla A (2014). Restricted nature of adult neural stem cells: re-
546 evaluation of their potential for brain repair. Front Neurosci 8: 162.
547

548 Oelschläger HHA, Oelschläger JS (2009) “Brain” in *Encyclopedia of Marine Mammals*, II edition,
549 ed. W.F. Perrin, B. Würsin and J.G.M. Thewissen. (Academic Press, San Diego, USA), pp. 134-
550 149.

551

552 Oelschläger HHA (2008) The dolphin brain - A challenge for synthetic neurobiology. *Brain Res*
553 *Bull* 75: 450-459.

554

555 Parolisi R, Peruffo A, Messina S, Panin M, Montelli S, Giurisato M, Cozzi B, Bonfanti L (2015)
556 Forebrain neuroanatomy of the neonatal and juvenile dolphin (*T. truncatus* and *S. coeruleoalba*).
557 *Front Neuroanat* 9: 140.

558

559 Patzke N, Spocter MA, Karlsson KÆ, Bertelsen MF, Haagensen M, Chawana R, Streicher S,
560 Kaswera C, Gilissen E, Alagaili AN, Mohammed OB, Reep RL, Bennett NC, Siegel JM, Ihunwo
561 AO, Manger PR (2015) In contrast to many other mammals, cetaceans have relatively small
562 hippocampi that appear to lack adult neurogenesis. *Brain Struct Funct* 220: 361-383.

563

564 Peretto P, Merighi A, Fasolo A, Bonfanti L (1997) Glial tubes in the rostral migratory stream of the
565 adult rat. *Brain Res Bull* 42: 9-21.

566

567 Peretto P, Giachino C, Aimar P, Fasolo A, Bonfanti L (2005) Chain formation and glial tube
568 assembly in the shift from neonatal to adult subventricular zone of the rodent forebrain. *J Comp*
569 *Neurol* 487: 407-427.

570

571 Peretto P, Bonfanti L (2014) Major unsolved points in adult neurogenesis: doors open on a
572 translational future? *Front Neurosci* 8:154.

573

574 Ponti G, Obernier K, Guinto C, Jose L, Bonfanti L, Alvarez-Buylla A (2013) Cell cycle and lineage
575 progression of neural progenitors in the ventricular-subventricular zones of adult mice, Proc Nat
576 Acad Sci USA 110, E1045-E1054.

577

578 Ponti G, Aimar P, Bonfanti L (2006a) Cellular composition and cytoarchitecture of the rabbit
579 subventricular zone (SVZ) and its extensions in the forebrain. J Comp Neurol 498: 491-507.

580

581 Ponti G, Peretto P, Bonfanti L (2006b) A subpial, transitory germinal zone forms chains of neuronal
582 precursors in the rabbit cerebellum. Dev Biol 294: 168-180.

583

584 Ridgway SH, Demski LS, Bullock TH, Schwanzel-Fukuda M (1987) The terminal nerve in
585 odontocete cetaceans. Ann NY Acad Sci 519: 201-212.

586

587 Ridgway SH (1990). The central nervous system of the bottlenose dolphin. In: The Bottlenose
588 Dolphin, S. Leatherwood, R.R. Reeves (Eds.), Academic Press (USA), pp. 69-97.

589

590 Rolando C, Parolisi R, Boda E, Schwab ME, Rossi F, Buffo A (2012) Distinct roles of Nogo-a and
591 Npogo receptor 1 in the homeostatic regulation of adult neural stem cell function and neuroblast
592 migration. J Neurosci 32: 17788-17799.

593

594 Rose KD (2006) The beginning of the age of mammals. JHU Press.

595

596 Sahay A, Wilson DA, Hen R (2011) Pattern separation: a common function for new neurons in
597 hippocampus and olfactory bulb. Neuron 70: 582-588.

598

599 Sakamoto M, Kageyama R, Imayoshi I (2014) The functional significance of newly born neurons
600 integrated into olfactory bulb circuits. *Front Neurosci* 8: 121.
601

602 Sanai N, Nguyen T, Ihrie RA, Mirzadeh Z, Tsai H-H, Wong M, Gupta N, Berger MS, Huang E,
603 Garcia-Verdugo JM, Rowitch DH, Alvarez-Buylla A (2011) Corridors of migrating neurons in the
604 human brain and their decline during infancy. *Nature* 478: 382-386.
605

606 Sanai N et al. (2004) Unique astrocyte ribbon in adult human brain contains neural stem cells but
607 lacks chain migration. *Nature* 427: 740-744.
608

609 Thewissen JG, Williams EM, Roe LJ, Hussain ST (2001) Skeletons of terrestrial cetaceans and the
610 relationship of whales to artiodactyls. *Nature* 413: 277-281.
611

612 Tong, CK, Alvarez-Buylla A (2014) Snapshot: adult neurogenesis in the V-SVZ. *Neuron* 81: 220-
613 220.
614

615 Tramontin AD, Garcia-Verdugo JM, Lim DA, Alvarez-Buylla A (2003) Postnatal development of
616 radial glia and the ventricular zone (VZ): a continuum of the neural stem cell compartment. *Cereb*
617 *Cortex* 13: 580-587.
618

619 Vadoaria KC, Gage FH (2014) Snapshot: adult hippocampal neurogenesis. *Cell* 156: 1114.
620

621 von Bohlen O, Halbach O (2011) Immunohistological markers for proliferative events, gliogenesis,
622 and neurogenesis within the adult hippocampus. *Cell Tissue Res* 345: 1-19.
623

624 Wang C, Liu F, Liu YY, Zhao CH, You Y, Wang L, Zhang J, Wei B, Ma T, Zhang Q, Zhang Y,
625 Chen R, Song H, Yang Z (2011) Identification and characterization of neuroblasts in the
626 subventricular zone and rostral migratory stream of the adult human brain. Cell Res 21: 1534-1550.
627
628
629
630

631

632 **Figure legends**

633

634 **Figure 1.** Animals and brain tissue samples used in this study (see also Table 1 and Parolisi et al.,
635 2015). A, Ten specimens belonging to two species of dolphins (*T. truncatus*, Tt; *S. coeruleoalba*,
636 Sc) at different ages (same colours as in B) were used. B, Arrow, coronal cutting direction to obtain
637 thick brain slices (examples on the right). ID, identification numbers; L, left hemisphere; R, right
638 hemisphere. Coloured lines indicate the amount of tissue available for
639 histological/immunohistochemical analyses in each animal and hemisphere (neonatal Tt, shades of
640 blue; adult Tt, shades of green; adult Sc, yellow), as a percentage of the whole brain extension
641 (black backclot; not in scale).

642

643 **Figure 2.** Tissue blocks analysed at different brain levels in all animals and ages (colors explained
644 in Fig. 1B).

645

646 **Figure 3.** Identification of an SVZ-like region (SVZ-lr) in the neonatal dolphin brain (*T. truncatus*)
647 and internal controls based on cell populations typically identified by DCX, CR, and Ki-67 antigen
648 in cerebral and cerebellar cortices of the same animals. A, Actively proliferating granule cell
649 precursors in the external germinal layer (EGL) of neonatal, as an internal control for Ki-67 antigen;
650 GL, granule cell layer; ML, molecular layer. B, Cortical neurons as an internal control for DCX (see
651 Bonfanti and Nacher, 2012) and calretinin (CR). C, No signs of residual germinal layer are
652 detectable along the lateral ventricle wall (1). General features reminiscent of the terrestrial
653 mammal SVZ are recognizable in a very small region (2), comprised between caudate nucleus
654 (CN), corpus callosum (CC) and ventricular corner: cell masses composed of tightly-packed cells
655 (Cm, asterisks) are surrounded by a dense, GFAP+, Vim+ astrocytic glial meshwork (Gm); Gm and

656 Cm form the area referred to as SVZ-lr (dotted line on the left; green area on the right). T, thalamus;
657 Cx, cortex; ic, internal capsule; scwm, subcortical white matter. Scale bars: 50 μ m.

658

659 **Figure 4.** Histological and immunocytochemical characterization of the SVZ-lr in neonatal and
660 adult dolphins (*T. truncatus* and *S. coeruleoalba*). A, Topographical position of the Cms (small red
661 dots, left), their profile (red areas, middle), and their detailed neuroanatomical location (right) at
662 different anterior-posterior brain levels. Cms are indicated by arrowheads in CrV stained sections
663 and by asterisks in immunofluorescence images; most of the small, tightly-packed cells are DCX+
664 and are surrounded by a GFAP+ astrocytic glial meshwork (Gm, green in the schematic drawings
665 on the right, illustrating the compartmentalized architecture of the SVZ-lr); CN, caudate nucleus; T,
666 thalamus; LV, lateral ventricle; bv, blood vessels. B, Same analyses carried out on brains of adult
667 animals, in both species; the profile of the Cms is black, since no DCX staining is detectable in their
668 cells. C, Left, anterior-posterior extension of the SVZ-lr in the neonatal dolphin (not showed in
669 adults since very similar); in blue, the lateral ventricle. Right, absolute and relative size of the
670 dolphin SVZ-lr and its Cms (absolute size: areas measured on 33 sections for neonates and 12
671 sections for adults; relative size: % absolute area with respect to coronal brain slice area; analysed at
672 L2) at different ages; the SVZ-lr is slightly enlarged in adults whereas the Cms are substantially
673 unchanged. Scale bars: A, 200 μ m (right bottom, 50 μ m); B, left, 1000 μ m; right, 50 μ m.

674

675 **Figure 5.** Estimation of neurogenic activity in the SVZ-lr and surrounding parenchyma of neonatal
676 (A, C left, D) and adult (C, right) dolphins. A, Left, no particular density of astrocytic cells forming
677 the glial meshwork (Am) is detectable close to the ventricular wall (the darker area is an optical
678 effect due to thickness of the brain section; see inset); middle and right, a few scattered dividing
679 cells revealed by Ki-67+ nuclei are detectable in the whole SVZ-lr area of neonatal dolphins,
680 randomly distributed in the Cms, at their limits or in the Gm. B, Quantification of proliferating cell
681 density in the dolphin SVZ-lr, subcortical white matter (ScWM), and corpus callosum (Cc) at

682 different ages; squares indicate the areas analysed; cell division rate is very low in the SVZ-lr of
683 neonates, substantially matching that in the parenchymal tissue (middle), being 34 fold lower than
684 in the cerebellar external germinal layer (EGL) and 62 fold lower than in the SVZ of neonatal mice
685 (right). No cell division is detectable in adults (graphically represented in F). C, At all ages and
686 species, in the SVZ-lr both compact (c) and less compact (lc) cell masses (Cm) are present, the
687 latter also harboring large cells with neuronal morphology (right, blue arrows). CN, caudate
688 nucleus; CrV, cresil violet; bv, blood vessels. D, Clusters of tightly-packed, DCX+ cells in the
689 ScWM surrounding the SVZ-lr in neonatal dolphins; their size and compactness is variable in
690 different individuals. After serial analysis at different brain levels (E, right; see Table 3), clusters
691 were confined within the ScWM and no one can be ever found in direct contact with the SVZ-lr (or
692 its Cms), a gap always existing between the most inner clusters and the SVZ-lr perimeter (F, left).
693 No DCX+ cell clusters are detectable in the white matter of adults (F, right). Scale bars: A left,
694 middle, 100 μm , right, 30 μm , insets, 10 μm ; C left, 50 μm , others, 10 μm ; D, 20 μm .

695

696 **Figure 6.** Cellular organization of the Cms in the dolphin SVZ-lr at different ages (A, left and B,
697 left bottom: neonate; A, right, B, top and right bottom: adult). A, Only scattered, small round-
698 shaped cells are DCX+ in a Cm of a neonatal dolphin (left), and none in the adult (right). B, Most
699 cells with large cell bodies found in the SVZ-lr are MAP2+ neurons (B, left, top and bottom; see
700 also A, right); a smaller amount of neurons is CR+, showing more differentiated shapes in adults,
701 including neurite extensions (B, right, top and bottom). C, Schematic representation of the cell types
702 in the dolphin SVZ-lr at different ages: small, round-shaped cells in the Cms show an overall loss of
703 DCX staining shifting from young to adult ages; neurons are already present around birth, although
704 showing less mature morphologies than in the adult (*T. truncatus*). Scale bars: 20 μm .

705

706 **Figure 7.** SVZ-lr and neurogenesis in dolphins at different ages: comparison with terrestrial
707 mammals. A, Several features displayed by the SVZ-lr of neonatal and adult dolphins converge to

708 the conclusion that their periventricular neurogenesis is almost exhausted at birth then being absent,
709 with progressive neuronal differentiation occurring within the SVZ-lr itself. Green, glial meshwork;
710 red, DCX+ cells; grey, DCX-negative cells; yellow dots, cell proliferation; ScWM, subcortical
711 white matter. B, Striking contrast between the typical proliferative, neurogenic SVZ of terrestrial
712 mammals and the non-neurogenic SVZ-lr of dolphins. C, Evolutionary considerations and
713 hypotheses: dolphins are cetaceans devoid of olfaction which derive from terrestrial mammals
714 endowed with olfactory structures (wolf-sized *Pakicetus*, Thewissen et al., 2001; Kishida et al.,
715 2015); an SVZ-lr (intended as an anatomical region) has been retained in extant dolphins, yet losing
716 any neurogenic capacity.

717
718
719

720 **Table 1.** Detail of the sampled bottlenose dolphins. C.E., Controlled environment.
 721
 722

Specimen	ID	Sex	Origin	Length/Weight	Age
<i>T. truncatus</i>	186	F	C.E.	110,5 cm/19kg	(neonatal) 19 days
	145	M	C.E.	118 cm/19kg	(neonatal) 9 days
	144	M	C.E.	117 cm/22,1kg	(neonatal) 9 days
	229	M	C.E.	99 cm/19 kg	(neonatal) 7 days
	343	F	C.E.	95 cm	(neonatal) 1 day
	344	M	Stranded	195 cm/98,5 Kg	Subadult
	192	F	Stranded	240 cm/178,5 kg	Adult
	196	M	Stranded	300 cm/219 kg	Adult
	319	M	Stranded	310 cm	Adult
<i>S. coeruleoalba</i>	167	M	Stranded	198 cm/94 kg	Adult

723
 724
 725

726
727
728

Table 2. Antibodies tested in this study, not working on our dolphin tissues.

Antigen	Antibody/antiserum	Host	Dilution	Source
BLBP	poly	rabbit	1:1000	Chemicon
Calbindin	poly	rabbit	1:10000	Swant
Calbindin	mono	mouse	1:1000	Swant
Cd11b	mono	mouse	1:1000	Sigma
DCX	poly	guineapig	1:800	Millipore
GABA	poly	rabbit	1:2000	Sigma
GFAP	mono	mouse	1:100	Millipore
GST	poly	rabbit	1:500	MBL
Iba 1	poly	rabbit	1:1000	Wako
IIIBtub	poly(Tuj1)	rabbit	1:1000	Covance
IIIBtub	mono (Tuj1)	mouse	1:100	Millipore
Ki-67	mono	mouse	1:300	BD Pharmigen
Ki-67	mono	mouse	1:200	Dako
Laminin	poly	rabbit	1:800	Dako
Map5	poly	goat	1:600	Santa Cruz
Map5	Mono	mouse	1:1500	Chemicon
MBP	mono	mouse	1:100	Millipore
NeuN	mono, A60	mouse	1:200	Millipore
Neurofilament	poly	rabbit	1:800	AbCam
Ng2	mono	mouse	1:200	Chemicon
Ng2	mono	mouse	1:300	US Biological
Ng2	mono	mouse	1:200	Upstate
Ng2	mono	mouse	1:200	Sigma
Ng2	poly	rabbit	1:400	Chemicon
Olig2	poly	goat	1:400	R&D System
Olig2	poly	rabbit	1:500	Millipore
PVim	poly	ra	1:800	AbCam
Parv19	mono	mouse	1:2000	Swant
Parv19	poly	rabbit	1:3000	Sigma
Pax 2	mono	mouse	1:800	Santa Cruz
Pax6	poly	rabbit	1:800	AbCam
PDGFRA	poly	rabbit	1:1000	Santa Cruz
PDGFRA	poly	rat	1:100	BD Pharmigen
PH3	poly	rabbit	1:500	Millipore
PH3	mono	mouse	1:300	Millipore
PSA NCAM	mono	mouse	1:900/1:2000	Biocampare
RIP	mono	mouse	1:400	Chemicon
S100B	poly	rabbit	1:3000	Swant
S100B	mono	mouse	1:10000	Sigma
Sox10	poly	goat	1:800	AbCam
Sox2	poly	rabbit	1:1000	Millipore
Sox2	poly	goat	1:400	Santa Cruz
Sox9	poly	rabbit	1:1000	Millipore
Tbr1	mono	mouse	1:600	AbCam
Tbr2	poly	rabbit	1:800	Millipore
Tenascin C	poly	rabbit	1:500	AbCam

729
730
731
732
733
734
735
736
737
738
739

740
741
742

Table 3. Step intervals (μm) between cryostat tissue sections used for different types of analysis within and outside the SVZ-Ir of the dolphin brains (see Fig. 2).

Species <i>Age</i>	Brain level	SVZ-like region				ScWM and Cc	
		Cm (CrV)	Gm (GFAP)	Cm (DCX)	Cell proliferation (Ki-67)	ScWM clusters (CrV, DCX)	Cell proliferation (Ki-67)
<i>Tt</i> <i>Neonate</i>	2	400	400	400	800	600	800
	3	400	200	200	400	400	400
	4	300	200	200	400	200	400
	5	300	400	400	400	200	400
	6	320	400	400	420	200	420
	7	320	400	400	420	400	420
	8	320	400	400	420	400	420
	9	400	400	400	800	600	600
10	400	400	400	800	600	800	
<i>Tt</i> <i>Adult</i>	2	800	1800	1200	2000	1200	1200
	3	400	1800	800	2000	800	800
	4	400	1800	800	2000	1000	1000
<i>Sc</i> <i>Adult</i>	3	400	1800	800	2000	1200	1200
	4	400	1800	800	2000	800	800
	5	400	1800	1200	2000	1000	1000
Analysed sections		879	633	738	459	1194	811

743
744
745
746
747
748

Tt, *T. truncatus*; *Sc*, *S. coerulealba*; Cm, periventricular cell mass; Gm, glial meshwork; ScWM, subcortical white matter; Cc, corpus callosum; CrV, cresil violet; DCX, doublecortin; GFAP, glial fibrillary acidic protein.

749 **Table 4.** Cellular and molecular features of the SVZ-lr in neonatal (1 day and 7-9 days) and adult *T.*
 750 *truncatus*.
 751
 752

Species age	Brain level	Cell masses (Cm)				Astrocytic meshwork (Am)		Ki-67+ cells (cells/mm ²)
		Number	Total area (μm ²)	DCX	N	GFAP	Area (μm ²)	
Tt <i>Neonatal</i> (1 day)	L2	11-10	139204,69±50298,49	+	+	+	2915883,33 ±128405,96	28,17±10,30
	L3	12-4	203093,03±38014,69	+	+	+	2235382 ±270675,11	n.d.
	L5	7-3	120030,02±51137,13	+	+	+	1141864,60 ±435986,77	20,07±10,05
Tt <i>Neonatal</i> (7-9 days)	L1	6-4	53028,95±20979,75	+	-	+	n.d.	n.d.
	L2	5-3	64972,45±25643,77	+	-	+	452090,11±87860,12	n.d.
	L3	3-1	158851,38±84676,47	+	+	+	876197,75±24983,08	78,57±84,52
	L4	2-6	91068,19±13325,03	+	+	+	688922,50±142514,73	31,35±5,20
	L5	2-6	118389,6 ±27084,12	+	-	+	4705096 ±1893947	56,55±22,45
Tt <i>Adult</i>	L2	6-8	222255,90 ±2218,19	-	+	+	7145366,66 ±783523,72	No cells
	L3	4-8	217682,52 ±6467,73	-	+	+	6044218 ±778629,68	
	L4	7-5	65976,75 ±29580	-	+	+	4621066,66 ±1570835,62	

753
 754
 755